

METHODOLOGY

Open Access



Deep-float salinity data synthesis for deep ocean state estimation: method and impact

Shuhei Masuda*, Satoshi Osafune and Tadashi Hemmi

Abstract

The importance of deep ocean observations has been recognized with regard to changes in the deep ocean such as global bottom-water warming. Therefore, sustainable deep ocean monitoring networks that use autonomous profiling floats have been widely proposed, and a number of deep-float deployment initiatives have begun around the world. Deployed floats promise to provide unprecedented deep ocean information. However, present deep-float data are known to have biases. In particular, a depth-dependent bias in salinity data is a major issue that prevents us from constructing global deep ocean monitoring networks. This paper proposes a new approach to utilize ongoing deep-float salinity data to reduce the bias in estimates of the global full-depth ocean state. It reports results from comparative experiments with and without deep-float data by using the proposed approach to examine the impact of data from currently operating deep floats on ocean state estimates. The results demonstrate that available float data possibly contribute local corrections to the modeled climate ocean state. Furthermore, we clarify how interannual basin-scale estimations are controlled by available deep-float salinity data in two specific regions of the Southern and Indian Oceans.

Introduction

The deep ocean has gained attention from climate researchers since Fukasawa et al. (2004) documented bottom-water warming in the abyssal North Pacific Ocean. The warming was detected by repeated high-accuracy ship-based observations by the World Ocean Circulation Experiment (WOCE) Hydrographic Program on its P1 survey line across the subarctic Pacific along 47° N, and Johnson et al. (2008) reported similar bottom-water warming in the Indian basin, also from revisit cruises. Subsequent researchers have detected global bottom-water warming (e.g., Purkey and Johnson 2010, Kouketsu et al. 2011).

Recent observational studies have indicated that Antarctic Bottom Water (AABW) has been freshening in some observational sections (e.g., Aoki et al. 2005, Rintoul 2007, Jacobs and Giulivi 2010). Purkey and Johnson (2013) quantified the freshening of AABW around Antarctica in a straightforward way. Nevertheless, deep ocean observations remain too sparse to resolve the temporal evolution of the deep ocean state.

At the beginning of the 2000s, dramatic progress was made in ocean observations with the introduction of Argo profiling floats capable of continuously monitoring ocean properties in the upper 2000 m (e.g., Argo Science Team, 2001). The success of the monitoring network for the upper ocean (e.g., Riser et al. 2016) motivates the construction of a similar global monitoring network for the deep ocean.

Recently, several types of deep floats have been developed or released. Among these, Deep NINJA is a reliable deep float that can continuously monitor depths to 4000 m as an extension of the conventional Argo float (Kobayashi et al. 2013). Deep NINJAs have been deployed in the North Pacific, South Indian, and Southern Oceans. Although interesting information about the deep ocean state has been obtained, it is known that the salinity measurements are sometimes biased by $O(0.01)$ mainly because of the conductivity sensor measurements, which makes it difficult to exploit them (Kobayashi 2016). Such bias is also found in measurements of other types of deep floats (e.g., Zilberman and Maze 2015).

In this paper, we propose a practical technique to blend these problematic but scientifically valuable data into full-depth ocean state estimates (e.g., Osafune et al.

* Correspondence: smasuda@jamstec.go.jp
Research and Development Center for Global Change, Japan Agency for Marine-Earth Science and Technology (JAMSTEC), Yokosuka, Japan

2015) by reducing their bias through a dynamical approach. Then, we examine the impact of available Deep NINJA data on deep ocean state estimation by comparing two data sets from a set of comparative experiments with and without the deep-float data.

Methods experimental

Data and assimilated system

The deep-float data that we used were 316 profiles obtained from available Deep NINJA floats collected and released by the Japan Agency of Marine-Earth Science and Technology (JAMSTEC: <http://www.jamstec.go.jp/ARGO/deepninja/>). Figure 1 shows the 17 Deep NINJA trajectories that were used in this study, covering the Southern (11 floats), North Pacific (4), and South Indian (2) Oceans (Table 1), each profile including temperature, salinity, and pressure. The equipped sensor accuracy was 0.002 °C for temperature and 0.005 for salinity. The data were processed through basic quality control in the same way as for a conventional Argo float (Wong et al., 2018).

Deep NINJA salinity data are known to have a bias that depends on pressure. Kobayashi (2018) thoroughly examined the bias in Appendix B of his paper. The problem is that the bias is different for each float; the values range from -0.005 to -0.02 at depths of 3500–4000 m based on analysis of float data for which there are also comparable ship-based Conductivity Temperature Depth profiler (CTD) data obtained at the same time as the float deployments (Fig. 2; Kobayashi 2016). We assume the bias value to be time independent since float lifetime is relatively short with a maximum of approximately 2 years (Table 1). This assumption may be premature since it has not yet been validated, so there could be some kind of time-dependent bias. Nevertheless, here, we assume there

is not as a first step toward improved deep ocean state estimation.

The data synthesis system is based on the work of Osafune et al. (2015). It generates a dynamically self-consistent long-term ocean state estimation, “Estimated STATE of global Ocean for Climate research” (ESTOC), by applying a four-dimensional variational (4D-VAR) adjoint approach (e.g., Sasaki 1970, Stammer et al., 2002, Wunsch and Heimbach 2007). The ocean general circulation model we used has a horizontal resolution of 1° in both latitude and longitude, and it includes 46 vertical levels for the global ocean basin. The control variables are surface forcing data and initial conditions for three-dimensional temperature and salinity distributions.

The ESTOC system is quite suitable for data synthesis of relatively sparse observations because the 4D-VAR adjoint method can generate a dynamically self-consistent state estimation through backward tracking of adjoint sensitivity (e.g., Köhl and Stammer 2004, Masuda et al. 2010), which takes advantage of both statistical and dynamical connections between the model and observations (e.g., Wunsch and Heimbach 2013). Thus, we used this system to examine the impact of available and locally distributed deep-float salinity data on deep ocean state estimation through a comparative twin experiment.

The other observations that were synthesized are similar to those in Osafune et al. (2015): subsurface temperature and salinity from the ENSEMBLES (EN4) dataset compiled by the Hadley Centre of the UK Meteorological Office (Good et al. 2013), sea surface temperature (SST) from historical 10-day datasets compiled from the Optimally Interpolated SST (OISST) dataset (Reynolds et al. 2002), and the historical 10-day sea surface dynamic height anomaly (SSDHA) derived

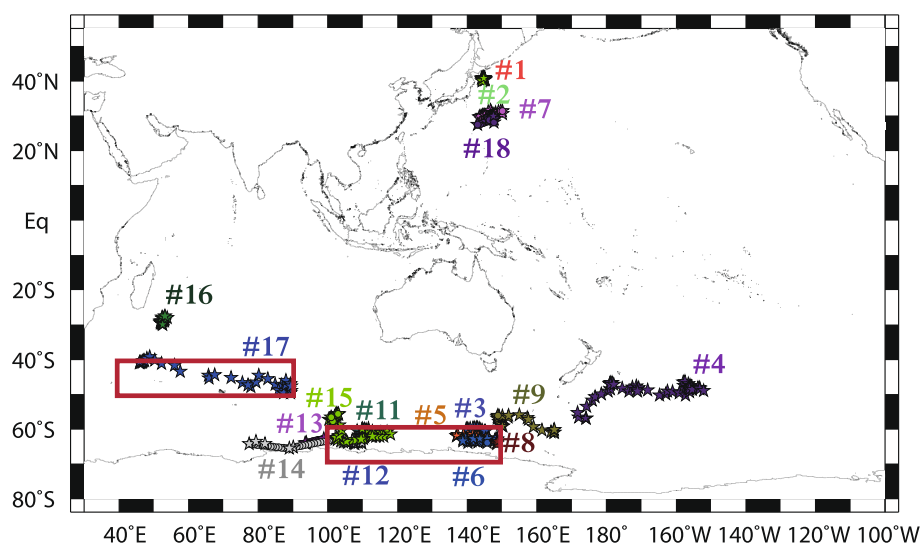


Fig. 1 Trajectories of the Deep NINJA floats listed in Table 1. Red rectangles show the analytical areas for Figs. 4 and 5 (see the text for more details)

Table 1 Inventory of Deep NINJA floats used in this study including information on the deployment and total number of observed profiles

| Serial no. | Date of deployment | Date of the last observation | Area of deployment | Position of deployment | No. of profiles |
|------------|--------------------|------------------------------|----------------------------------|-----------------------------|-----------------|
| 1 | 2012/8/29 | 2012/8/30 | Subarctic, North Pacific | 40° 40.00' N, 114° 46.18' E | 1 |
| 2 | 2012/8/29 | 2012/8/29 | Subarctic, North Pacific | 40° 40.00' N, 114° 46.18' E | 16 |
| 3 | 2012/12/19 | 2013/5/31 | Off the Adélie Coast, Antarctica | 60° 00.62' S, 139° 56.12' E | 9 |
| 4 | 2012/12/5 | 2012/12/5 | South of NZ, Southern Ocean | 56° 59.87' S, 173° 59.42' E | 25 |
| 5 | 2012/12/17 | 2013/7/14 | Off the Adélie Coast, Antarctica | 62° 00.38' S, 137° 00.42' E | 10 |
| 6 | 2012/12/16 | 2014/8/22 | Off the Adélie Coast, Antarctica | 62°45.73' S, 143° 36.05' E | 23 |
| 7 | 2013/7/17 | 2013/7/17 | Subtropical, North Pacific | 30° 03.91' N, 144° 58.09' E | 33 |
| 8 | 2014/3/6 | 2014/3/27 | Off the Adélie Coast, Antarctica | 63° 40.55' S, 148° 35.65' E | 3 |
| 9 | 2014/3/7 | 2014/3/7 | Off the Adélie Coast, Antarctica | 59° 14.34' S, 150° 08.85' E | 23 |
| 11 | 2014/1/19 | 2014/1/19 | Off the Budd Coast, Antarctica | 60° 03.50' S, 109° 53.32' E | 10 |
| 12 | 2014/1/22 | 2014/1/22 | Off the Budd Coast, Antarctica | 62° 00.42' S, 110° 00.19' E | 5 |
| 13 | 2014/1/27 | 2014/1/27 | Off the Budd Coast, Antarctica | 64° 15.90' S, 107° 42.00' E | 24 |
| 14 | 2014/1/24 | 2014/1/24 | Off the Budd Coast, Antarctica | 64° 05.36' S, 109° 51.01' E | 40 |
| 15 | 2014/12/6 | 2014/12/6 | Off the Budd Coast, Antarctica | 59° 59.96' S, 109° 51.92' E | 43 |
| 16 | 2016/1/31 | 2016/1/31 | Western Indian Ocean | 29° 59.98' S, 52° 32.01' E | 18 |
| 17 | 2016/2/2 | 2016/2/2 | Western Indian Ocean | 40° 41.49' S, 45° 54.43' E | 20 |
| 18 | 2016/3/2 | 2016/3/2 | Subtropical, North Pacific | 29° 56.31' N, 147° 27.26' E | 12 |

from sea surface height data in the Copernicus Marine Environment Monitoring Service (CMEMS) dataset. In addition, we used a global mean sea level reconstructed through the method of Church and White (2011), which is updated and provided by the Commonwealth Scientific and Industrial Research Organisation (CSIRO). The

EN4 dataset includes some Deep NINJA data only for water temperature.

Dynamical approach to bias reduction of salinity data

There are many studies on observation bias correction (e.g., Eyre 1992, Zhu et al. 2014, Eyre 2016). Here, we propose a pre-process for biased Deep NINJA salinity data. This is a kind of “static scheme” in which the statistics of the differences between observations and model background equivalents are evaluated to remove biases (Eyre 2016). The advantage of our method is the use of time-dependent ocean states based on an archived ocean observation dataset to calculate the statistics.

First, the Deep NINJA data were compiled as monthly gridded data averaged over each model grid volume. Then, we compared the salinity profiles from each gridded Deep NINJA with the observation-based background ocean state of a time-varying (monthly) reference field. The state was made by a conventional optimal interpolation of a monthly gridded EN4 dataset based on the World Ocean Atlas 2013 (WOA13) produced by the National Oceanographic Data Center. The EN4 dataset included Argo float data together with quality-controlled available observations. In particular, the number of profiles in the Southern Ocean greatly increased after 2008 (not shown).

Since deep floats drift freely with the ocean currents, the reference ocean state should be determined region-by-region, depth-by-depth, and month-by-month. The depth-dependent salinity bias value b can thus be

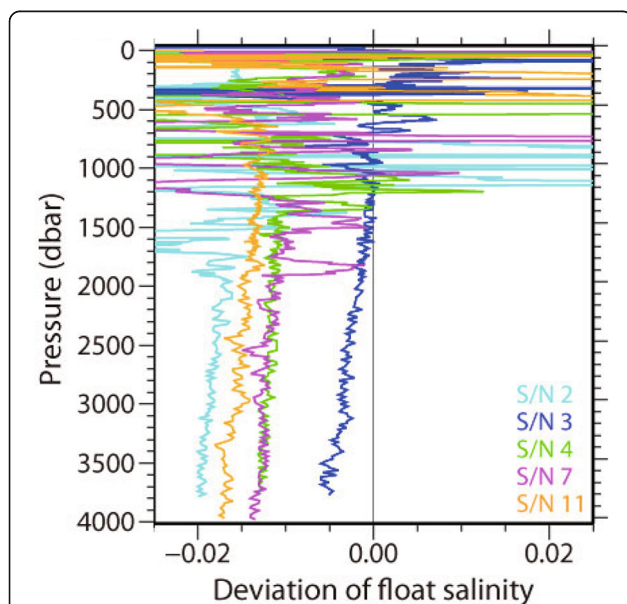


Fig. 2 Depth profiles of the deviation of float salinity from shipboard reference CTD observations cited from Kobayashi (2016). The colors identify the Deep NINJA floats with serial numbers 2, 3, 4, 7, and 11 listed in Table 1

defined as a function dependent only on depth (z) for each float as

$$b(z) = \overline{y(t, r(t)) - y_{\text{ref}}(\text{mon}(t), r(t))},$$

where y is the salinity profile value of the float observation, t the time, $r(t)$ the three-dimensional float position, y_{ref} the monthly background ocean state, and $\text{mon}(t)$ the month relevant to the observation time t . The overbar denotes the time-mean procedure for the period during which each float operates. The procedure means we calculate the average value of the differences between the reference ocean state and float observation along the float trajectory for each depth from the surface to 4000 m under the assumption that both observational mean values match each other.

The depth-dependent salinity bias was determined by the above approach for each float. The values at 4000 m depth range from -0.044 to 0.003 (Fig. 3 a, b) shows the estimated mean bias profile with standard deviations. The values at depths of 3500 and 4000 m are -0.015 and -0.017 , respectively. The standard deviation values are 0.008 and 0.009 , respectively for each depth. The magnitude of the bias increases as the depth increases beyond 2000 m.

Besides bias, there are other factors that could contribute to the differences between the reference ocean states and float observations, for example, sampling error and representativeness error. Although we cannot evaluate either of them, the gross features of Fig. 3a are largely consistent with those of Fig. 2 (and Kobayashi 2018) where negative biases of order 0.01 with standard deviations of order 0.005 were detected at 3500–4000 m depth when compared with shipboard

CTD observations performed when several Deep NINJAs were deployed. This partly validates our methodology. Further examination by using more in situ data will be required to test and improve our approach. In addition, our scheme has some limitations due to the fact that the statistics depend only on a priori available information. Some update of the bias correction scheme, for instance, by using a variational scheme which are adaptive rather than static ones (e.g., Derber and Wu, 1998; Zhu et al. 2014), should lead to further refinement.

We used the salinity values for each float, with the individual depth-dependent bias values removed, as observational values in the ESTOC system. The ESTOC system is based on an anomaly data assimilation method that automatically determines the weight of observational mean values to observational time-varying components by using the statistical values of model variables (Eq. (2) of Osafune et al. 2015). We assume that corrected Deep NINJA data are reliable with regard to variability. Then, the assimilation approach of Osafune et al. (2015) reduces to conventional anomaly assimilation for the compiled Deep NINJA dataset. In addition, we place weight on synthesizing the Deep NINJA data by taking into consideration the observational number included in each profile and the accuracy of the observation. We assume 80 observation levels are included in one deep-ocean grid whose height is approximately 400 m. Deep NINJA sensors have about 2.5 times greater accuracy than gridded EN4 salinity data, which we estimate from averaged EN4 standard deviation values from 2012 to 2016 in the world’s oceans at a depth of 4000 m. The total weight may be somewhat overestimated due to differences in the statistics between EN4 and Deep NINJA data. We discuss this point below.

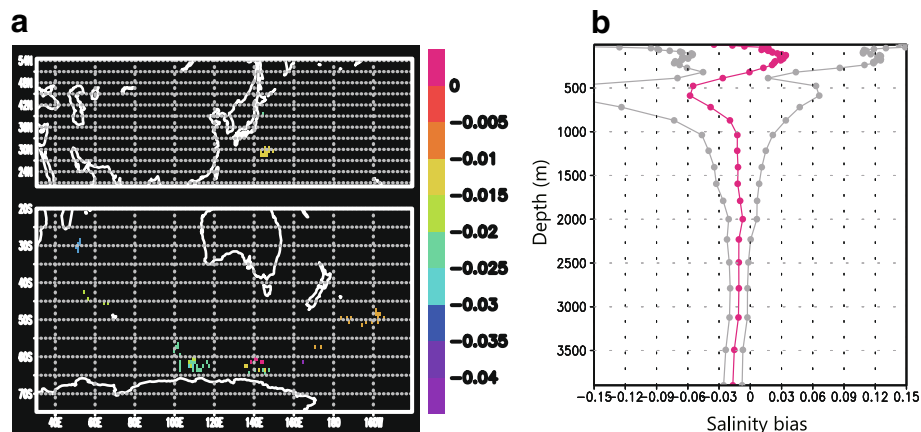


Fig. 3 a Estimated salinity bias at 4000 m depth for each float in Fig. 1. b Depth profile of the estimated mean salinity bias for all 17 Deep NINJA floats. The error area is defined by one standard deviation (gray lines) calculated from the 17 profiles

Comparative state estimations to examine deep-float impact

We carried out two data synthesis experiments on the Earth Simulator parallel supercomputer of JAMSTEC to obtain ocean state estimations with and without deep-float data. The case without deep-float data, hereafter called the reference case, is the same as in Osafune et al. (2015), except for the length of the assimilation window (2000–2016) and implementation of global mean sea-level data assimilation. The deep-float case (hereafter, DN case) is the same as the reference case but includes Deep NINJA salinity data for the period 2012–2016 (Table 1), synthesized through the proposed data process and anomaly assimilation described in the “Dynamical approach to bias reduction on salinity data” section. The ocean state estimation was obtained after 50 iterations. The period of analysis in this paper is from

2007 to 2016 to focus on the impact of deep float observations.

Results and discussion

Local impact of deep-float salinity data

To examine the temporal development of the estimated subsurface ocean state, we focus on two areas of 50° longitude by 10° latitude (Fig. 1): the Southern Ocean area off Antarctica’s Wilkes Land (100–150° E, 60–70° S) and the South Indian Ocean area (40–90° E, 40–50° S). The former is an area of concentrated monitoring over 5 years (Table 1), while the latter is an area covered by only two floats for a 1-year period.

Figure 4 shows the temporal development of salinity at 3500 m depth for the period 2012–2016. The area

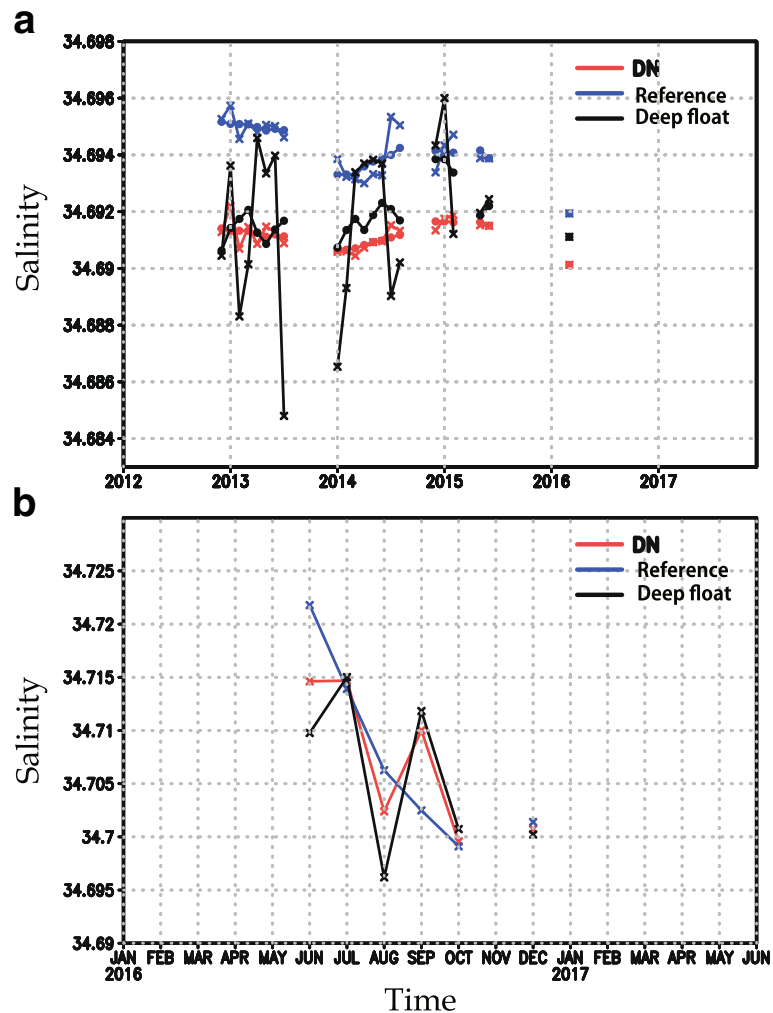


Fig. 4 Temporal development of area-mean salinity at 3500 m depth for **a** the Southern Ocean area (100–150° E, 60–70° S) and **b** the South Indian Ocean area (40–90° E, 40–50° S), outlined in Fig. 1. The black lines indicate deep-float observations, and the blue and red lines denote the reference and DN cases, respectively, averaging only where deep-float observations exist (see the text for more details). Crosses denote monthly values and dots denote 6-month running mean values

average is determined for the grid points and times where deep-float observations exist. For the Southern Ocean, the results for the DN case tend to follow the deep-float data closely. The root mean square difference values are reduced to 0.0013 compared to 0.003 for the reference case values for the 6-month running mean (black dots in Fig. 4a). The raw values of the deep-float observations (crosses in Fig. 4a) generally have larger variances than the state estimations. This is mainly because these include variability at a scale smaller than the model grid size of 1°. For the Indian Ocean, the root mean square difference is reduced to 0.0033 compared to 0.0075 for the reference case values (crosses in Fig. 4b). Although the differences between the results for the DN case and deep-float observations are less than the initial sensor accuracy of 0.005, these corrections can be meaningful since data synthesis reduces errors through integration of other information. These subtle

but systematic reductions of the differences demonstrate the potential importance of deep-float observations for estimating the tempo-spatially “local” deep ocean state. That is, available deep-float salinity data can contribute to local ocean state estimation by providing a control variable, although our approach is an empirical one that includes some assumptions.

Representativeness of float observations

We further investigated the tempo-spatial representativeness of float observations for most of the above areas and time-windows by using estimated states. Figure 5 is the same as Fig. 4, but the area average of the reference and DN cases is shown for all grid points included in the area, resulting in temporally continuous curves.

For the Southern Ocean, the estimated deep ocean state shows a salinity trend of 0.002 per decade (red line in Fig. 5a), which appears consistent with bias-corrected

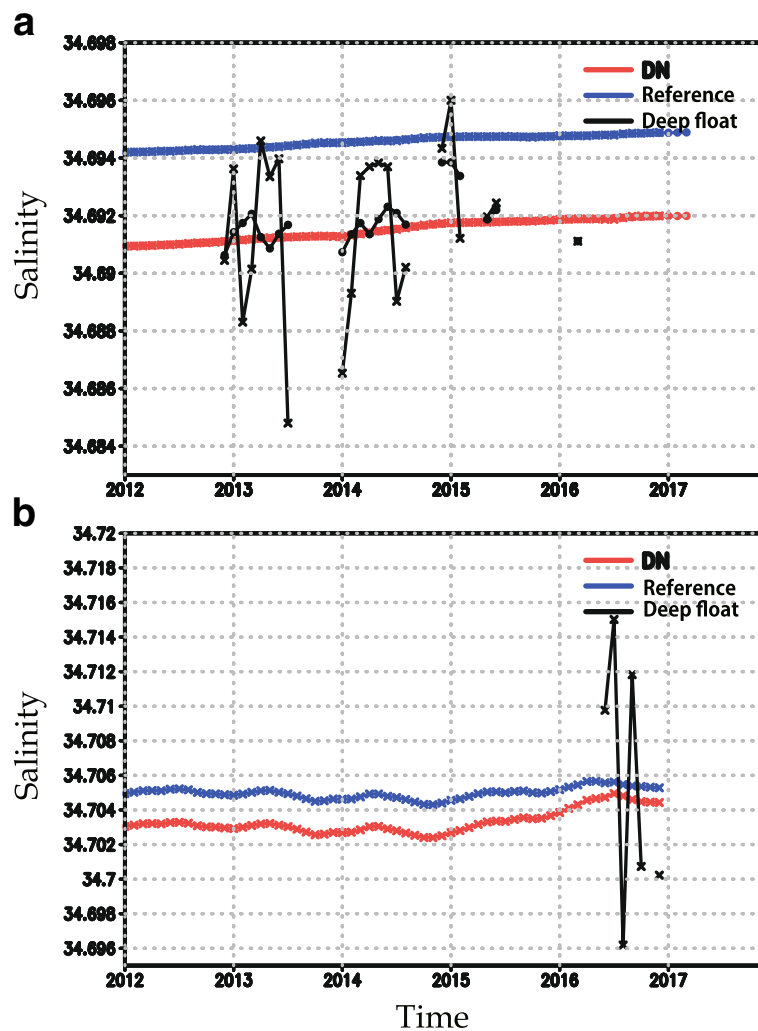
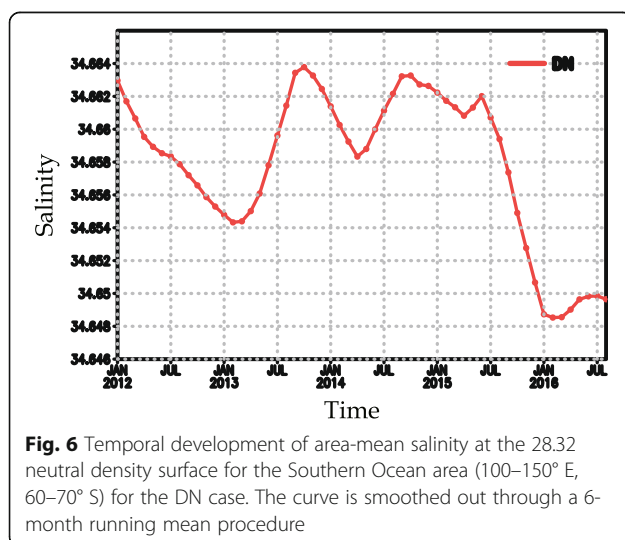


Fig. 5 The same as Fig. 4a and b for **a** and **b**, except that the area averages of the reference and DN cases are determined for all the grid points within each analytical area

deep-float observations (black dots). This result suggests that monthly mean gridded salinity values from sparse deep-float data can represent the salinity in the entire target area to some extent, which demonstrates that it is possible for ongoing deep-float observation to control the modeled deep ocean state even for a relatively large area. Note that the well-known freshening in this region (e.g., Purkey and Johnson 2013; Kobayashi 2018) is visible when the time series are replotted with a neutral density coordinate as in Kobayashi (2018; Fig. 6), although our anomaly data assimilation makes neutral density values of the mean state shift to lighter ones.

For the Indian Ocean, the impact of deep-float data is limited to the past 2 years, before which only the baseline is shifted. This result implies that two deep-float deployments during 1-year periods for this area can contribute only one more year of correction by adjoint retro-chronic temporal development. Longer-term deep ocean climate state estimation requires more data even for short periods of 1-year monitoring since the adjoint signal itself can be traced back for a period of 50 years (e.g., Masuda et al. 2010).

It should be noted that this observational density (number of deep floats and monitoring periods: ten deployments during 5 years for the Southern Ocean and two deployments during 1 year for the Indian Ocean) does not provide precise indices for a global monitoring scheme for some ocean state estimations. This is because the obtained quantitative impacts can depend highly on the local ocean state, period, model representativeness of each region, data assimilation schemes, and other factors. In addition, some issues remain to be solved in the data processing. For example, the monthly background ocean state used as a reference field in the data processing basically works to exclude the detection of long-term trends.



Another problem is that of weight validation in data synthesis. We made another state estimation in which the weight of the Deep NINJA data synthesis was reduced by 95%. The root mean square difference values for the Southern Ocean area, discussed in the “[Local impact of deep-float salinity data](#)” section, change to 0.0018 from 0.0013 for the case of Fig. 4a, consistently reducing compared to 0.003 for the reference case values for the 6-month running mean (not shown). For the Indian Ocean, the root mean square difference changes to 0.0059 from 0.0033 for the case of Fig. 4b, also reducing compared to 0.0075 for the reference ones (not shown). This shows that a relatively small weight can still result in certain corrections and may suggest that further iteration possibly leads to a closer solution. Nevertheless, how we should determine the weight remains to be solved.

Our estimation is a practical first step toward a better deep-float observation scheme by using the present deep floats. Further research along these lines will provide indispensable information for the construction of future deep-ocean monitoring systems and, in addition, the improvement of the deep floats themselves inclusive of equipped sensors as well as data assimilation systems.

Conclusions

We have proposed a practical technique of deep-float salinity data processing for deep ocean state estimation to explore deep ocean climate change. The method consists of preprocessing for reduction of bias with a dynamical approach suitable for anomaly data assimilation under some assumptions.

We examined the impact of deep-float salinity data on ocean state estimation by using a 4D-VAR data synthesis system and proposed data processing in target regions in the Southern Ocean and Indian Ocean. The results show that corrected deep-float data can help constrain the modeled ocean state around the specific localities of float profiles. Regarding basin-scale climate change, in the case of the Southern Ocean, where we made concentrated observations with ten floats over 5 years, a slight salinization trend was estimated for the entire 50° longitude by 10° latitude area, basically in agreement with bias-corrected deep-float data. In the case of the South Indian Ocean where only two floats were available for a 1-year period, no significant change in time development was found until 1 year before data input.

Although these results do not provide concrete indices for either the required float number or the deployment period due to the limited sampling, they can contribute to global deep-float network planning in the near future by demonstrating the controllability of the modeled deep ocean state.

Acknowledgements

We thank Dr. Kanako Satoh, Mr. Fumihiko Akazawa, Ms. Mizue Hirano, and Mr. Tetsuharu Iino for their technical support. We are also thankful for the valuable comments and suggestions of Dr. Taiyo Kobayashi, Dr. Shigeki Hosoda, Dr. Nozomi Sugiura, and Mr. Toshimasa Doi. Figure 2 was kindly provided by Dr. T. Kobayashi. Numerical calculations were performed on the Earth Simulator of JAMSTEC. This work was partly supported by a Grant-in-Aid for Scientific Research on Innovative Areas (MEXT KAKENHI-JP15H05817/JP15H05819) and JSPS KAKENHI Grant 17H04579. WOA13 data were provided by the NOAA National Centers for Environmental Information from its website at <https://www.nodc.noaa.gov/OC5/woa13/>. The CMEMS altimeter products were obtained from <http://marine.copernicus.eu/>.

Funding

This work was done by management expenses grants for Japan Agency for Marine-Earth Science and Technology (JAMSTEC), and was partly supported by a Grant-in-Aid for Scientific Research on Innovative Areas (MEXT KAKENHI-JP15H05817/JP15H05819) and JSPS KAKENHI Grant 17H04579.

Availability of data and materials

Deep float data used in this study are available through our website [<http://www.jamstec.go.jp/ARGO/deepninja/>]. Original real-time data are released by Argo network [http://www.argo.ucsd.edu/Argo_Project_Office.html] through Japanese Argo Data Assembly Center. A recent version of global ocean state estimation is published from repository site [<http://www.godac.jamstec.go.jp/estoc/e/index.html>].

Authors' contributions

SM analyzed the data and wrote the paper. SO proposed the basic concept of quality control and helped in the coding of FORTRAN. TH compiled the float data and supported numerical experiments. All authors read and approved the final manuscript.

Competing interests

The authors declare that they have no competing interests.

Publisher's Note

Springer Nature remains neutral with regard to jurisdictional claims in published maps and institutional affiliations.

Received: 26 July 2018 Accepted: 2 December 2018

Published online: 29 December 2018

References

- Aoki S, Rintoul SR, Ushio S, Watanabe S, Bindoff NL (2005) Freshening of the Adélie Land Bottom Water near 140°E. *Geophys Res Lett* 32:L23601. <https://doi.org/10.1029/2005GL024246>
- Argo Science Team (2001) In: Koblinsky CJ, Smith NR (eds) Argo: the global array of profiling floats, in observing the oceans in the 21st century. GODAE Project Office, Bureau of Meteorology, Melbourne, pp 248–258
- Church JA, White NJ (2011) Sea-level rise from the late 19th to the early 21st century. *Surv Geophys* 32:585–602
- Derber JC, Wu WS (1998) The use of TOVS cloud-cleared radiance in the NCEP SSI analysis system. *Mon Weather Rev* 126:2287–2299. [https://doi.org/10.1175/1520-0493\(1998\)126<2287:TUOTCC>2.0.CO;2](https://doi.org/10.1175/1520-0493(1998)126<2287:TUOTCC>2.0.CO;2)
- Eyre JR (1992) A bias correction scheme for simulated TOVS brightness temperatures, Technical Memorandum. ECMWF, Reading, UK, p 176
- Eyre JR (2016) Observation bias correction schemes in data assimilation systems: a theoretical study of some of their properties. *Q J R Meteorol Soc* 142(699): 2284–2291. <https://doi.org/10.1002/qj.2819>
- Fukasawa M, Freeland H, Perkin R, Watanabe T, Uchida H, Nishina A (2004) Bottom water warming in the North Pacific Ocean. *Nature* 427:825–827. <https://doi.org/10.1038/nature02337>
- Good SA, Martin MJ, Rayner NA (2013) EN4: quality controlled ocean temperature and salinity profiles and monthly objective analyses with uncertainty estimates. *J Geophysical Res Oceans* 118:6704–6716. <https://doi.org/10.1002/2013JC009067>
- Jacobs SS, Giulivi CF (2010) Large multidecadal salinity trends near the Pacific–Antarctic continental margin. *J Clim* 23:4508–4524. <https://doi.org/10.1175/2010JCLI3284.1>
- Johnson GC, Purkey SG, Bullister JL (2008) Warming and freshening in the abyssal southeastern Indian Ocean. *J Clim* 21:5351–5363
- Kobayashi T (2016) Deep NINJA observation. Seventeenth Argo Steering Team Meeting Document 7(2):1–12 http://www.argo.ucsd.edu/DeepNINJA_AST17.pdf
- Kobayashi T (2018) Rapid volume reduction in Antarctic Bottom Water off the Adélie/George V Land coast observed by deep floats. *Deep Sea Res*, in press. <https://doi.org/10.1016/j.dsr.2018.07.014>
- Kobayashi T, Watanabe K, Tachikawa M (2013) Deep NINJA collects profiles down to 4,000 meters. *Sea Technol* 54(2):41–44
- Köhl A, Stammer D (2004) Optimal observations for variational data assimilation. *J Phys Oceanogr* 34(3):529–542. <https://doi.org/10.1175/2513.1>
- Kouketsu S, Doi T, Kawano T, Masuda S, Sugiura N, Toyoda T, Igarashi H, Kawai Y, Katsumata K, Uchida H, Fukasawa M, Awaji T (2011) Deep ocean heat content changes estimated from observation and reanalysis product and their influence on sea level change. *J Geophys Res* 116:C03012. <https://doi.org/10.1029/2010JC006464>
- Masuda S, T. Awaji, N. Sugiura, J. P. Matthews, T. Toyoda, Y. Kawai, T. Doi, S. Kouketsu, H. Igarashi, K. Katsumata, H. Uchida, T. Kawano, M. Fukasawa, 2010: Simulated rapid warming of abyssal North Pacific waters, *Science*, 329, 322–327. doi:<https://doi.org/10.1126/science.1188703>
- Osafune S, Masuda S, Sugiura N, Doi T (2015) Evaluation of the applicability of the Estimated Ocean State for Climate Research (ESTOC) dataset. *Geophys Res Lett* 42(12):4903–4911
- Purkey SG, Johnson GC (2010) Warming of global abyssal and deep Southern Ocean waters between the 1990s and the 2000s: contributions to global heat and sea level rise budgets. *J Clim* 23:6336–6351
- Purkey SG, Johnson GC (2013) Antarctic Bottom Water warming and freshening: contributions to sea level rise, ocean freshwater budgets, and global heat gain. *J Clim* 26:6105–6122. <https://doi.org/10.1175/JCLI-D-12-00834.1>
- Reynolds RW, Rayner NA, Smith TM, Stokes DC, Wang W (2002) An improved in situ and satellite SST analysis for climate. *J Clim* 15(13):1609–1625
- Rintoul SR (2007) Rapid freshening of Antarctic Bottom Water formed in the Indian and Pacific oceans. *Geophys Res Lett* 34:L06606. <https://doi.org/10.1029/2006GL028550>
- Riser SC, Freeland HJ, Roemmich D et al (2016) Fifteen years of ocean observations with the global Argo array. *Nat Clim Chang* 6:145–153
- Sasaki Y (1970) Some basic formalisms in numerical variational analysis. *Mon Weather Rev* 98:875
- Stammer D, Wunsch C, Fukumori I, Marshall J (2002) State estimation in modern oceanographic research. *EOS* 83(27):289–294–295
- Wong A, Keeley R, Carval T, and Argo Data Management Team: Argo Quality Control Manual for CTD and Trajectory Data 2018, doi:<https://doi.org/10.13155/33951>
- Wunsch C, Heimbach P (2007) Practical global oceanic state estimation. *Physica D–Nonlinear Phenomena* 20:197–208. <https://doi.org/10.1016/j.physd.2006.09.040>
- Wunsch C, Heimbach P (2013) Dynamically and kinematically consistent global ocean circulation and ice state estimates. In: Siedler G, Church J, Gould J, Griffies S (eds) Ocean circulation and climate: a 21st century perspective. Chapter, vol 21. Elsevier, pp 553–579. <https://doi.org/10.1016/B978-0-12-391851-2.00021-0>
- Zhu Y, Derber J, Collard A, Dee D, Treadon R, Gayno G, Jung JA (2014) Enhanced radiance bias correction in the National Centers for Environmental Prediction's Gridpoint Statistical Interpolation data assimilation system. *Q J R Meteorol Soc* 140:1479–1492. <https://doi.org/10.1002/qj.2233>
- Zilberman N, and G. Maze, 2015: Report on the Deep Argo Implementation Workshop, <http://www.argo.ucsd.edu/DAIW1report.pdf>